

A Quad Element UWB MIMO Antenna Design for Indoor High Data Rate Communication

Saminathan Thiruvankadam*, Eswaran Parthasarathy and Aravindan Madhavan

Department of Electronics and Communication Engineering, SRM Institute of Science and Technology, Kattankulathur, Chennai, 603203, Tamilnadu, India

Received 18 July 2024; Accepted 14 December 2024

Abstract

This research presents a compact four-element Ultra-Wideband (UWB) MIMO antenna for indoor wireless applications. The dimensions of the antenna being suggested are $40 \times 40 \times 1.6 \text{ mm}^3$, which consists of U-slotted circular radiator with 50Ω microstrip feed line and optimized ground plane that have a slight edge cut. The top side of the substrate consists of four elements that are orthogonally placed, and the bottom side of the substrate consists of optimized ground planes. The designed antenna operating at 3.1- 13 GHz for indoor applications. Further, MIMO antenna characteristics parameters like $ECC < 0.004$, $TARC < -30 \text{ dB}$, Diversity Gain (DG) of almost 9.99 dB, CCL below 0.4 bits/Hz/sec have been analyzed. Further, the designed four port UWB antenna was validated for transmitting and receiving signal strength using NI USRP to verify the performance in an indoor environment real time.

Keywords: CCL DG, ECC, MIMO, TARC, UWB

1. Introduction

The need for fast wireless communication has prompted the development of diverse antenna technologies. In particular, ultra-wideband (UWB) technology has gained interest due to its ability to transmit data at high rates over short distances. The FCC's authorization of the unlicensed frequency band has increased the appeal of UWB technology in various wireless applications, making it a popular area of research among many professionals [1-2]. However, UWB technology operates in a frequency range that is shared with other wireless technologies, such as Wi-Fi and Bluetooth, which can cause interference and multi path fading.

To exploit the spatial diversity and multiplexing gains of the wireless channel, MIMO uses numerous antennas at both the transmitting and receiving ends. Antenna design is important in MIMO systems, as the antennas must be able to efficiently transmit and receive signals in a highly complex and dynamic environment. Therefore, there is a growing interest in the development of MIMO antenna technologies that can provide reliable and high-quality wireless communication.

In [3] the authors propose a two-port UWB-MIMO antenna design for use in wireless communication systems. The antenna design is based on a modified circular monopole structure with a dual band-notched characteristic. The two notched bands lie at 3.5 GHz and 5.5 GHz, which are commonly used for WiMAX and WLAN applications, respectively. The suggested antenna has a total size of $20 \times 20 \text{ mm}^2$. In [4] the article presents a unique four-port MIMO antenna for multi-standard automotive communications. The antenna design has two layers of PCB, with a decoupling structure and a switched feeding network that allows for reconfigurability in multiple frequency bands. In [5] the

author proposes a unique MIMO antenna layout of size $39 \times 39 \times 1.6 \text{ mm}^3$, that can be used in Ultra-wideband (UWB) applications. The antenna includes two square-slotted circular patches with a Defected Ground Structure (DGS) to reduce cross-coupling between the antennas. The UWB MIMO antenna employs four semi-angle radiator designs, as well as radiating elements with low mutational coupling and orthogonal positioning [6]. The Substrate Integrated Wave guide (SIW) technique is employed with a four-semi circle shaped UWB antenna [7]. In [8] the study introduces and explores a very small UWB-MIMO antenna with four rejected bands. Four bands are segregated by etching the radiators with four pairs of in-proportion L-shaped slots. In [9] this article presents a small, UWB-MIMO antenna that has two ports. The proposed antenna has an optimal dimension of $20 \times 20 \text{ mm}^2$. The suggested antenna offers mutual coupling of less than 25 dB, extended UWB bandwidth of 2-12 GHz. In [10] this research presents a dual band-notched compact two-port MIMO antenna of size $19 \times 30 \times 0.8 \text{ mm}^3$ overall operating in the UWB frequency range. Two identical radiating elements with an attached ground plane are arranged next to one another to form the MIMO antenna. The $90 \times 90 \times 1.6 \text{ mm}^3$ size ring-shaped radiator with less coupling in between each other for UWB/5G/WLAN band IoT applications [11]. In order to improve isolation between the radiators used a metal or dielectric periodic structure called the EBG configuration has band pass/stop properties and offers strong radiating element isolation [12-15]. Additionally, the geometric correction and additional structures such as parasitic element [16], neutralization line [17], short circuit pin [18], loading slot [19], meta material [20-24] are used to improve the isolation. From the literature survey, the various UWB antenna designs having a relatively large size and improved isolation used various techniques such as decoupling structure, defective ground plane structure, split ring resonator etc.

*E-mail address: samnatt@srmist.edu.in

ISSN: 1791-2377 © 2024 School of Science, DUTH. All rights reserved.

doi:10.25103/jestr.176.09

In this work, the designed four-port antenna has a compact size of $40 \times 40 \times 1.6 \text{ mm}^3$, which consists of U-slotted circular radiator with feed line and optimized ground plane that have a slight edge cut. The top side of the substrate consists of four elements that are orthogonally placed, and the bottom side of the substrate consists of optimized ground planes.

Features of suggested MIMO Antenna:

- The antenna operates in the frequency band 3.1 - 13 GHz for indoor applications.
- Further, MIMO antenna characteristics parameters like $ECC < 0.004$, $TARC < -30\text{dB}$, Diversity Gain (DG) of almost 9.99 dB, and CCL below 0.4 bits/s/Hz have been analyzed.
- The antenna parameters have shown the antenna as a strong contender for Indoor applications which has been verified by USRP 2943R.

2. Antenna Design

2.1 Single element design

The designed ultra-wide-band antenna design is illustrated in Figure 1. It consists of a U-shaped slotted circular radiator with a 50Ω feed line on the front side of the substrate, while the reverse side of the substrate has a partial ground plane with an optimized slight edge cut. The antenna is built on a FR4 substrate ($\epsilon_r = 4.4$, $\tan \delta = 0.02$) with a height of 1.6 mm. The antenna has dimensions of $16 \times 20 \text{ mm}^2$, and the optimized dimensions can be found in Table 1. The following Equation (1) can be used to calculate the circular radiator at the lowest operating frequency at 3.1 GHz [25]. The designed antenna resonates at the range 3.1 - 13 GHz as shown in the Figure 2. It is illustrated that $S_{11} < -10 \text{ dB}$ at the operating bandwidth.

$$f_r = \frac{c}{\gamma} = \frac{150}{2 \times (\pi \times b)g + w} = 3.1 \text{ GHz} \quad (1)$$

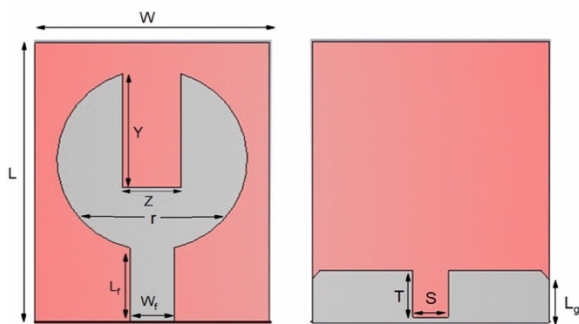


Fig. 1. Designed UWB unit cell

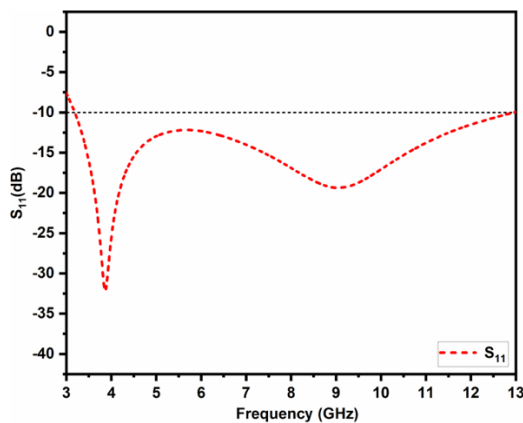


Fig. 2. Reflection coefficient (S_{11}) of designed antenna

2.2 Equivalent circuit of UWB antenna

To achieve wideband response in ultra-wideband antennas, a common approach is to cascade multiple LC resonators whose resonant frequencies continuously overlap. This allows for a broader frequency coverage compared to narrow band antennas, where a single LC resonant circuit is used as an approximation. By using multiple resonators in cascade, the antenna can effectively cover a wider range of frequencies, resulting in a broad-band response. This approach is commonly used in designing ultra-wideband antennas to achieve efficient and consistent performance across a wide frequency range.

Table 1. Dimension of designed antenna

Parameter	Dimensions(mm)
L	20
W	16
L_f	6.1
W_f	5
X	4
Y	8
Z	4
S	2.8
T	3.3
L_g	3.7
r	6.5

Software for applied wave research (AWR) is used, and the analogous circuit element is shown in Figure 3. The corresponding circuit's simulation result carried out in CST software is, compared to the prototypical simulation proposed in AWR software. The AWR software is used to create the antenna equivalent circuit which is the combination of resistors, inductors, and capacitors which are connected to each other using a wire and the corresponding values are mentioned in the below Table 2, after the combined component values have been used and tuned. It can be visualized from Figure 4, that the CST and AWR software results are in good agreement throughout the bandwidth [26]. The capacitance and inductance are calculated using Equations (2), (3) and (4).

$$L = \frac{img(Z_{11})}{2\pi f} \quad (2)$$

$$f = \frac{1}{(2\pi\sqrt{LC})} \quad (3)$$

$$C = \frac{1}{(2\pi f)^2 L} \quad (4)$$

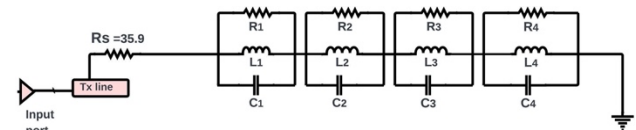


Fig. 3. Equivalent circuit model of UWB antenna

Table 2. RLC values of UWB antenna

S. No	Resistance (Ohm)	Inductance (pH)	Capacitance (pF)
1	$R_1 = 198.7$	$L_1 = 846$	$C_1 = 7.99$
2	$R_2 = 88.9$	$L_2 = 1356$	$C_2 = 6.75$
3	$R_3 = 12.62$	$L_3 = 71.9$	$C_3 = 3.01$
4	$R_4 = 24.39$	$L_4 = 76.529$	$C_4 = 2.651$

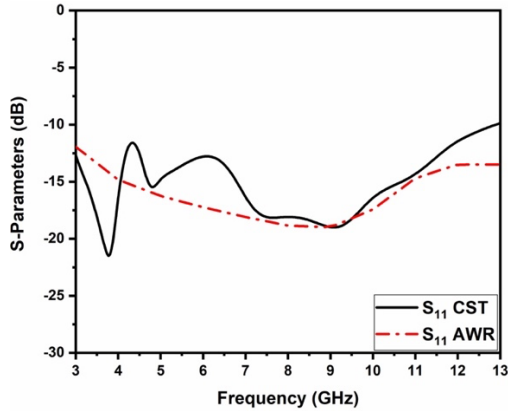


Fig. 4. Reflection coefficient (S_{11}) of UWB antenna compared with circuit model

2.3 MIMO implementation

The four port UWB MIMO antenna illustrated in Figure 5. It is perceived that the top side of the FR4 substrate consists of four elements that are placed orthogonally, and the reverse side consists of partial ground planes. The FR4 substrate is used which is a common choice for antenna design because it is not expensive and available. The suggested antenna structure has dimensions of 40 x 40 mm². The simulated S-Parameters of the proposed antenna as illustrated in Figure 6. It is observed that the reflection coefficient of the designed antenna $S_{11} < -10$ dB at the resonance frequency of 3.1 to 13 GHz. bandwidth. Furthermore, the mutual coupling of the proposed antenna lies below -18 dB at the entire operating bandwidth. Hence, the envisioned patch antenna demonstrates good impedance matching at all ports and high levels of isolation between ports.

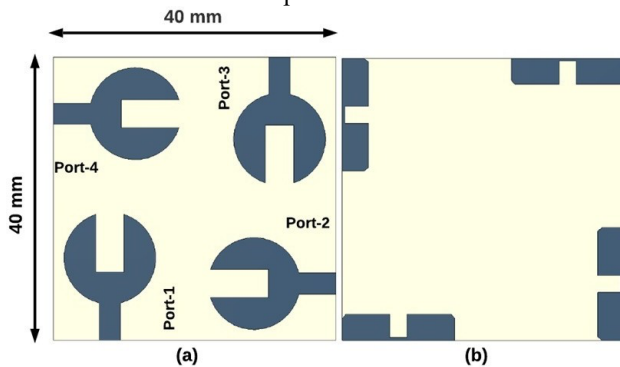


Fig. 5. Schematic diagram of design antenna a) Front side b) Back side

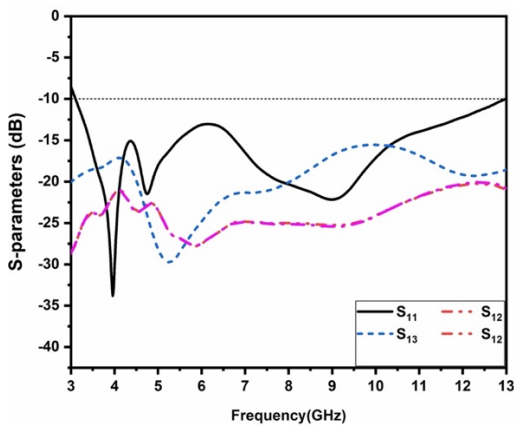


Fig. 6. S-parameters of the designed antenna

2.4 Surface Current Distribution

The surface current distribution of an antenna can provide information about the mutual coupling between two antennas.

When two antennas are in close proximity, they can interact with each other through their near fields, resulting in a mutual coupling effect. The surface current distribution of an antenna can show the intensity and direction of the current flowing on the surface of the antenna. The surface current distribution of the designed antenna is simulated at 3.4 GHz when port -1 to port-4 is excited as shown in coupling between the ports.

Figure 7(a)-(d). It is observed that when port -1 is activated other ports are disabled there is negligible current flow others ports. Therefore, the proposed antenna has low mutual GHz.

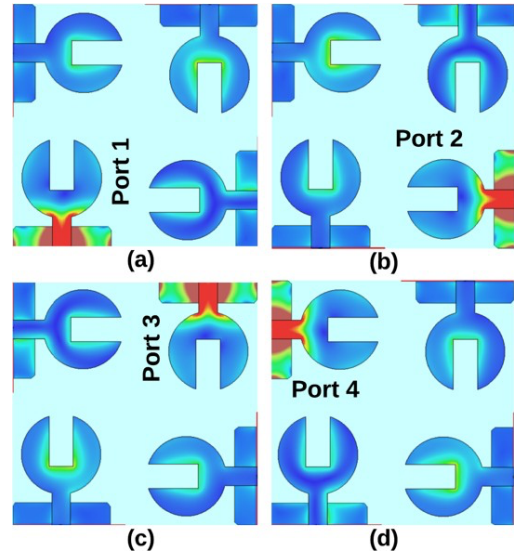


Fig. 7. Surface current distribution of proposed 4-port MIMO antenna when port-1 to port-4 excited at 3.4GHz

3. Experimental Results

The designed antenna S-parameters, radiation pattern, gain, and total efficiency are all detailed here. MIMO parametric analysis and real-time validation are also covered in this section.

3.1 S-parameters

The designed four port UWB MIMO antenna fabricated using FR4 substrate as demonstrated, and the measured S-parameter using the VNA (vector network analyzer) set-up is shown in Figure 8. Figure 9 compares the S-parameter values of measured and simulated results. It was revealed that the S_{11} lie below -10dB between at 3.1 to 13 GHz. Further S_{12} , S_{13} , and S_{14} curves lie below -18 dB throughout the frequency band. The suggested antenna meets the -18 dB MIMO criterion which means that the antenna can be effectively used in MIMO systems to improve the system performance and radiate signals in a way that minimizes the amount of signal coupling between them. Therefore, the designed antenna is in accordance with simulated and measured results.

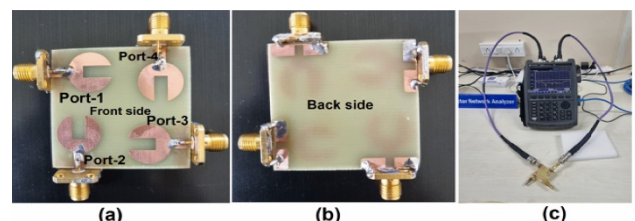


Fig. 8. Fabricated image of suggested UWB MIMO antenna measured using VNA

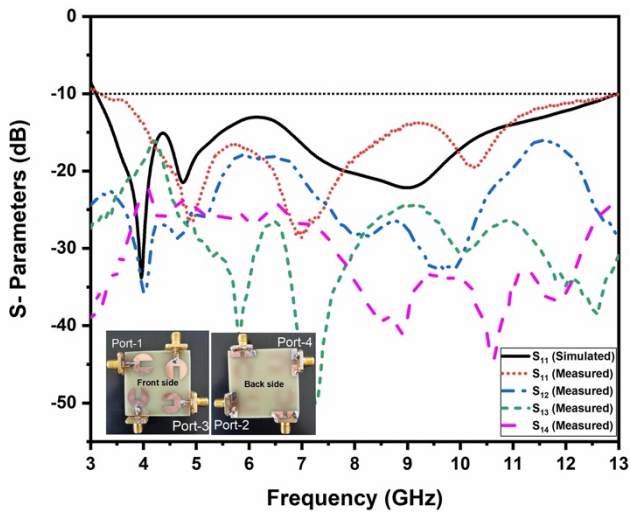


Fig. 9. The simulated S_{11} compared with measured S_{11} result and measured results of S_{12} , S_{13} , S_{14}

3.2 Radiation Pattern

The designed 4-port UWB MIMO antenna radiation patterns are measured using a highly absorbent anechoic chamber as shown in Figure 10. The E (x-y) and H (y-z) plane of designed UWB MIMO antenna are obtained at frequencies of 3.4GHz, 5.4 GHz, and 10.5 GHz, which are derived from experimental and simulated results as illustrated in Figure 11. It is perceived that the proposed antenna provides a nearly omnidirectional of co-polarization and cross-polarization radiation patterns of at the operating frequency. Hence, by observing the simulated and measured patterns, an omnidirectional behavior of the antenna can be detected which means uniform signal is radiated in all directions.

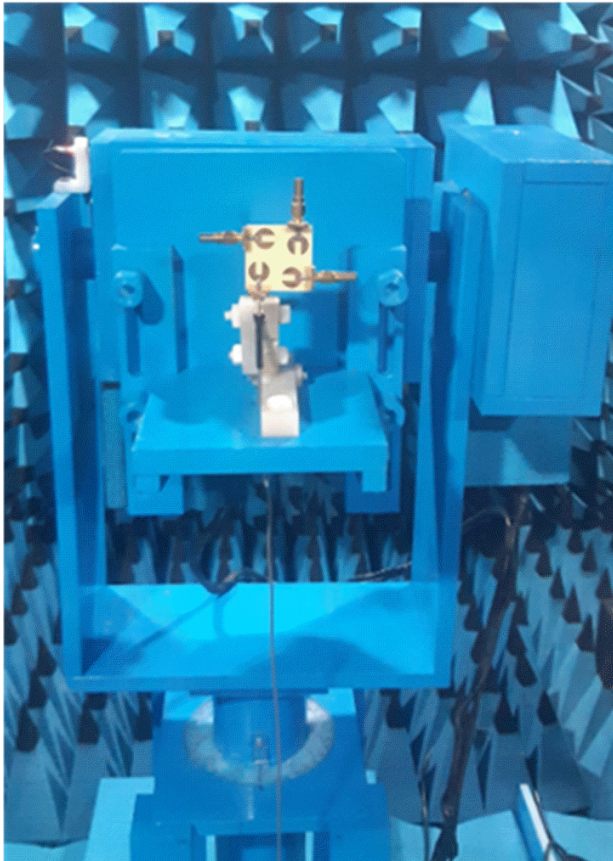


Fig. 10. Designed 4-port UWB MIMO antenna under test in anechoic chamber

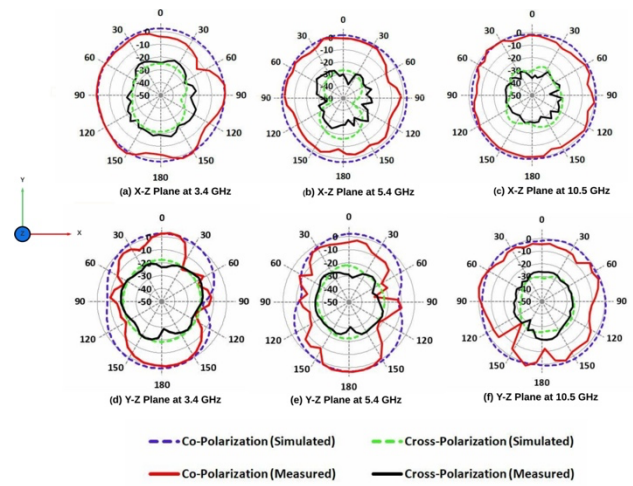


Fig. 11. Radiation pattern of designed 4-port UWB MIMO antenna co-polarization and cross-polarization at 3.4 GHz, 5.4 GHz, 10.5 GHz respectively

3.3 Gain and Total efficiency

The far-field gain and overall efficiency of the designed MIMO antenna at port 1 are shown Figure 12. It is perceived that the designed 4-port UWB MIMO at the 3.1-13 GHz of gain and total efficiency is 1.2 –6 dBi, 70-85 % respectively. Thus, the designed antenna is very effective in indoor applications.

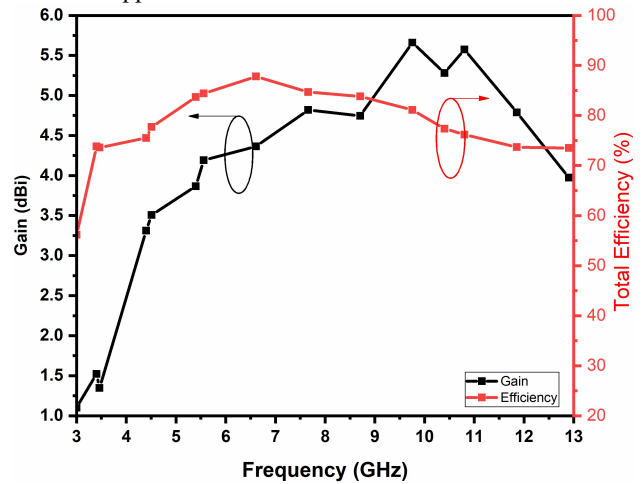


Fig. 12. Measured values of Gain and total efficiency

3.4 MIMO characterization

3.4.1 ECC

The Envelope Correlation Coefficient (ECC) is an estimate of the correlation among the amplitudes of the signals received by the distinct antennas in a multiple antenna system. It indicates the extent to which the signals received by the different antennas are similar or dissimilar in amplitude. In practical MIMO systems, a low ECC is desirable, as it indicates that the signals received by the antennas are uncorrelated, which can improve the diversity of the system and reduce interference. A high ECC, on the other hand, can lead to reduced performance and increased susceptibility to interference [27]. However, the real time ECC must be < 0.5 . The far-field based ECC of the antenna can be calculated using Equation (5).

$$ECC = \frac{\iint |\overline{s_a}(\theta, \varphi) \cdot \overline{s_b}(\theta, \varphi)|^2}{\iint |\overline{s_a}(\theta, \varphi)|^2 d\Omega \iint |\overline{s_b}(\theta, \varphi)|^2 d\Omega} \quad (5)$$

Figure 13 Shows the measured ECC value of the suggested antenna system. It was observed from the graph that the ECC remains below 0.004 throughout the operating bandwidth of 3.1-13 GHz.

3.4.2 DG

The Diversity gain (DG) of a MIMO antenna system refers to the increase in signal quality or performance that results from using multiple antennas to transmit and receive signals. Typically, a system equipped with multiple antennas can achieve greater diversity gain compared to a system with a single antenna. This is because the former can capitalize on the variations in the received signals to enhance the overall signal strength.

$$DG = 10 \sqrt{1 - ECC^2} \quad (6)$$

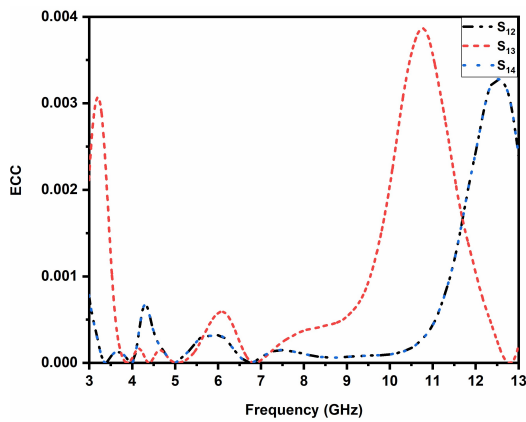


Fig. 13. ECC of proposed UWB MIMO antenna

The antenna's diversity gain can be calculated using the Equation (6). Figure 14 illustrated that the designed 4-port UWB MIMO antenna diversity gain. It is observed that DG is >9.98 at the entire operating bandwidth.

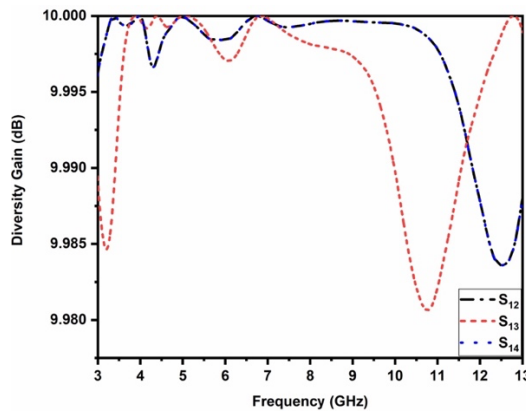


Fig. 14. Diversity gain of proposed UWB MIMO antenna

3.4.3 TARC

Total Active Reflection Coefficient (TARC) is an estimate of the effectiveness of a MIMO antenna system in transmitting and receiving signals. In a MIMO system, the signals from each antenna can interfere with each other, leading to reduced signal quality and performance. TARC is a measure of the degree of interference between the antennas. The two-port MIMO antenna can be calculated using the Equation (7)

$$TARC = \sqrt{\frac{(s_{11} + s_{12} e^{j\theta})^2 + (s_{21} + s_{22} e^{j\theta})^2}{2}} \quad (7)$$

Where, θ lies from 0 to 2π .

In general, a TARC value of less than 0 dB is considered good. From Figure 15, It can be visualized that the TARC value lies below -30 dB in the overall ultra-wide bandwidth.

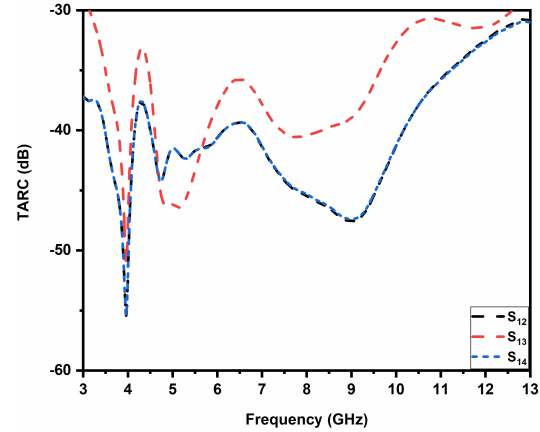


Fig. 15. TARC of proposed UWB MIMO antenna

3.4.4 CCL

In MIMO antenna systems, the ideal value of Channel Capacity Loss (CCL) is as low as possible, ideally zero, which would indicate no loss in channel capacity. A low CCL means that the MIMO system is able to take advantage of the multiple antennas to mitigate the effects of fading, interference, and noise, and improve the overall performance of the communication system. The permissible CCL values are CCL less than 0.4 bits/sec/Hz. The two-port MIMO antenna CCL values can be estimated using Equations (8) and (9).

$$CCL = -\log_2 \det[\Psi^R] \quad (8)$$

$$\Psi^R = \begin{pmatrix} \varphi_{11} & \varphi_{12} \\ \varphi_{21} & \varphi_{22} \end{pmatrix} \quad (9)$$

The measured value is shown in Figure 16, and from 3 to 13 GHz, the CCL value lies below 0.4 bits/s/Hz.

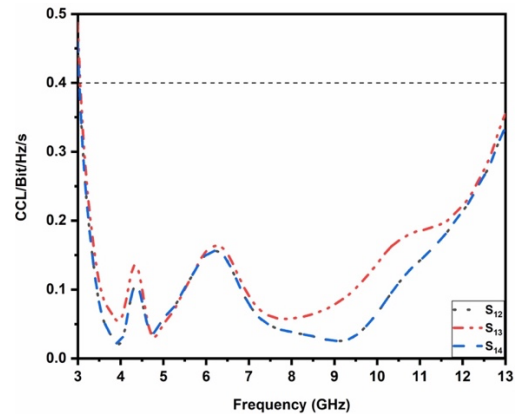


Fig. 16. CCL of proposed UWB MIMO antenna

3.5 Housing effect

This section evaluates the proposed performance of a four-port MIMO antenna in packaging. The antenna is located 10 mm below a copper sheet measurements $L_m \times W_m = 40 \text{ mm} \times$

40 mm. Figure 17 display the corresponding S-parameters (reflection coefficients and mutual coupling) of the suggested antenna. In the near-field region, it is observed that the suggested antenna maintains UWB performance even when positioned a copper sheet. Its reliable operation in indoor applications is thus confirmed by the fact that the copper sheet has no effect on antenna performance.

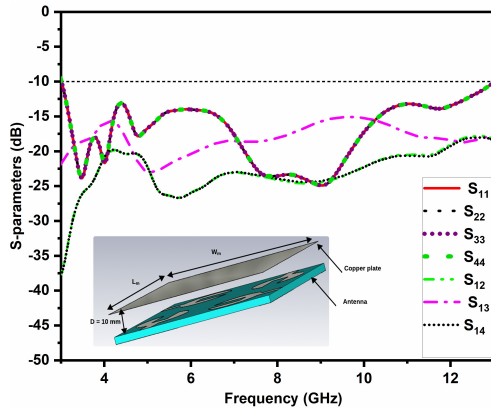


Fig. 17. S-parameters under the copper sheet

3.6 Comparison between existing MIMO antenna designs.

As shown in Table 3, the developed antenna parameters are compared to previous UWB MIMO antenna works.

Table 3. Comparison between existing MIMO antenna designs ref Antenna size (L x W in mm²)

Ref	Antenna size (L x W in mm ²)	Number elements	of	Operational band (GHz)	Mutual Coupling (dB)	ECC	Real time application
[8]	21 x 27	2		3 – 11	<-15	< 0.005	No
[9]	20 x 20	2		2 – 12	<-20	< 0.005	No
[10]	19 x 30	2		3.1 – 10.6	<-20	< 0.13	No
[11]	90 x 90	4		3.1 – 10.6	<-15	< 0.15	No
[22]	94.2 x 94.2	4		2 – 12	<-20	< 0.1	No
[23]	50 x 40	4		2.5 – 14	<-15	< 0.04	No
[24]	80 x 35	4		2.57 – 12	<-15	< 0.005	No
Proposed	40 x 40	4		3.1 - 13	<-18	< 0.004	Yes

Port-1 (A and E) and port-2 (B and F) of the antenna are connected as Tx, Port 3 (C and G), and Port 4 (D and H) are connected with the USRP-1 and USRP-2, as shown in Figure 19. NI USRP is set to trans/receive the signal frequency at 6 GHz. The received signal strength is < -15 dBm, which indicates that the antenna radiates much stronger than the minimum signal strength required (-40 dBm) for most wireless communication applications. The envisioned antenna is a strong contender for short-range indoor wireless applications such as Wi-Fi or Bluetooth

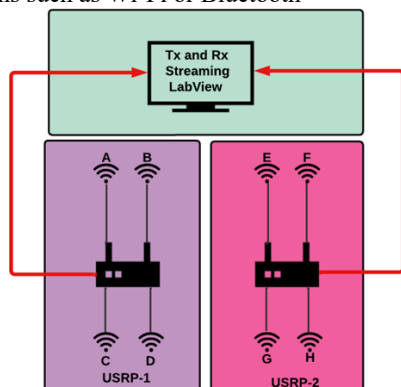


Fig. 18. Schematic diagram of the proposed UWB MIMO antenna in an indoor environment using USRP

- The size of the 4-port UWB MIMO antenna is smaller than that of [11, 22, 23, 24]
- The mutual coupling of the designed antenna is better than [8, 11, 23, 24] without use of any decoupling structure.
- The ECC of the designed antenna is lower than most of the previous works because of higher isolation.
- The proposed antenna has been tested in indoor applications compared previous works.

3.7 Antenna test in a real-time scenario using USRP in an indoor environment

The real-time short-range communication performance of the fabricated antenna was investigated using indoor base stations. The NI USRP is a versatile tool that can measure the signal quality of a proposed antenna. The USRP has been configured using the software LabVIEW to generate and analyse the signals, enabling the measurement of key performance metrics such as signal-to-noise ratio, bit error rate, modulation quality, and signal strength. The experimental setup consists of two NI USRP connected with the proposed antenna working as a transmitter and receiver integrated with the NI LabVIEW 802.11 framework. A schematic diagram of indoor base station signal transmission and reception employing the NI USRP 2943R and proposed UWB MIMO antenna is shown in Figure 18.

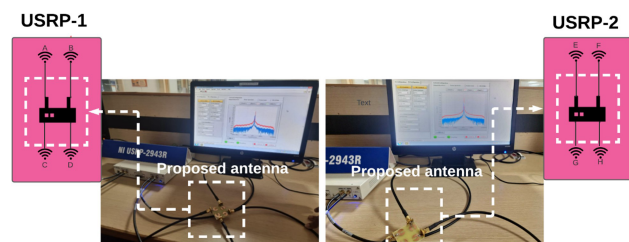


Fig. 19. Real Time testing of the antenna in indoor environment using NI USRP

4. Conclusion

A 4-port MIMO antenna has been developed, simulated, and examined in real-time using NI USRP in an indoor environment. The designed antenna consists of four circular radiators with a U slot with feed lines, and an optimized ground plane. The envisioned UWB antenna operates in a frequency band of 3.1 to 13 GHz. Significant antenna features including S11 lies below -10 dB, mutual coupling (S12, S13, S14) between the ports < -18 dB, omnidirectional radiation pattern is attained both co-polarization and cross-polarization. The MIMO parameters including, ECC < 0.004, TARC < -30 dB, CCL < 0.4 bits/sec/Hz, and diversity gain of

almost 10, follow well with the standard values. Overall, the compact size of antenna is suitable for indoor applications.

This is an Open Access article distributed under the terms of the Creative Commons Attribution License.



References

- [1] Mengyuan Lin and Zengrui Li, "A compact 4×4 dual band-notched UWB MIMO antenna with high isolation," in *2015 IEEE 6th Int Symp. Microw., Ant., Propag. EMC Techn. (MAPE)*, Shanghai, China: IEEE, Oct. 2015, pp. 126–128. doi: 10.1109/MAPE.2015.7510281.
- [2] Jian Ren, Wei Hu, Yingzeng Yin, and Rong Fan, "Compact Printed MIMO Antenna for UWB Applications," *Anten. Wirel. Propag. Lett.*, vol. 13, pp. 1517–1520, Jul 2014, doi: 10.1109/LAWP.2014.2343454.
- [3] A. Kumar, A. Q. Ansari, B. K. Kanaujia, J. Kishor, and S. Kumar, "An ultra-compact two-port UWB-MIMO antenna with dual band-notched characteristics," *AEU - Int. J. Electron. Commun.*, vol. 114, Feb. 2020, Art. no. 152997, doi: 10.1016/j.aeue.2019.152997.
- [4] B. Ramakrishnan and V. Murugiah Sivashanmugham, "Novel four-port reconfigurable filtering MIMO antenna for multi-standard automotive communications," *AEU - Int. J. Electron. Commun.*, vol. 146, Mar. 2022, Art. no. 154108, doi: 10.1016/j.aeue.2022.154108.
- [5] K. Sreeramulu, Sk. T. Mahaboob, R. R. Reddy, and K. L. Kishore, "A Square Slotted Circular Patch MIMO Antenna with DGS for UWB Applications," in *2022 Int. Conf. Comput., Commun. Power Techn. (IC3P)*, Visakhapatnam, India: IEEE, Jan. 2022, pp. 94–97. doi: 10.1109/IC3P52835.2022.00027.
- [6] A. A. R. Saad and H. A. Mohamed, "Conceptual design of a compact four-element UWB MIMO slot antenna array," *IET Microw., Ant. Propag.*, vol. 13, no. 2, pp. 208–215, Feb. 2019, doi: 10.1049/iet-map.2018.5163.
- [7] A. A. R. Saad, "Approach for improving inter-element isolation of orthogonally polarised MIMO slot antenna over ultra-wide bandwidth," *Electron. Lett.*, vol. 54, no. 18, pp. 1062–1064, Sep. 2018, doi: 10.1049/el.2018.5346.
- [8] L. Wu, X. Cao, and B. Yang, "Design and analysis of a compact UWB-MIMO antenna with four notched bands," *Progr. Electromagn. Res. M*, vol. 108, pp. 127–137, Feb. 2022, doi: 10.2528/PIERM21112101.
- [9] M. K. Sharma, M. Kumar, and J. P. Saini, "Design and Analysis of a Compact UWB-MIMO Antenna with Improved Isolation for UWB/WLAN Applications," *Wireless Pers Commun*, vol. 119, no. 4, pp. 2913–2928, Aug. 2021, doi: 10.1007/s11277-021-08378-3.
- [10] A. Kumar, A. Q. Ansari, B. K. Kanaujia, and J. Kishor, "Dual Circular Polarization with Reduced Mutual Coupling Among Two Orthogonally Placed CPW-Fed Microstrip Antennas for Broadband Applications," *Wireless Pers Commun*, vol. 107, no. 2, pp. 759–770, Jul. 2019, doi: 10.1007/s11277-019-06298-x.
- [11] R. Mathur and S. Dwari, "Frequency and port reconfigurable MIMO antenna for UWB / 5G / WLAN band IoT applications," *Int J RF Microw Comput Aided Eng*, vol. 31, no. 7, Jul. 2021, doi: 10.1002/mmce.22692.
- [12] Fan Yang and Y. Rahmat-Samii, "Reflection phase characterizations of the EBG ground plane for low profile wire antenna applications," *IEEE Trans. Antennas Propagat.*, vol. 51, no. 10, pp. 2691–2703, Oct. 2003, doi: 10.1109/TAP.2003.817559.
- [13] L. Zhao, D. Yang, H. Tian, Y. Ji, and K. Xu, "A pole and AMC point matching method for the synthesis of HSF-UC-EBG structure with simultaneous AMC and EBG properties," *Progr. Electrom. Res.*, vol. 133, pp. 137–157, Jan. 2013, doi: 10.2528/PIER12062406.
- [14] M. T. Islam and Md. S. Alam, "Compact EBG structure for alleviating mutual coupling between patch antenna array element," *Progr. Electrom. Res.*, vol. 137, pp. 425–438, Feb. 2013, doi: 10.2528/PIER12121205.
- [15] M. S. Sharawi, A. B. Numan, and D. N. Alofi, "Isolation improvement in a dual-band dual-element MIMO antenna system using capacitively loaded loops," *Progr. Electrom. Res.*, vol. 134, pp. 247–266, Nov. 2013, doi: 10.2528/PIER12090610.
- [16] A. Toktas and A. Akdagli, "Compact multiple-input multiple-output antenna with low correlation for ultra-wide-band applications," *IET Microw., Anten. Propag.*, vol. 9, no. 8, pp. 822–829, Jun. 2015, doi: 10.1049/iet-map.2014.0086.
- [17] M. S. Khan, A. Capobianco, M. F. Shafique, B. Ijaz, A. Naqvi, and B. D. Braaten, "Isolation enhancement of a wideband MIMO antenna using floating parasitic elements," *Micro & Optical Tech Letters*, vol. 57, no. 7, pp. 1677–1682, Jul. 2015, doi: 10.1002/mop.29162.
- [18] S.-W. Su, C.-T. Lee, and F.-S. Chang, "Printed MIMO-Antenna System Using Neutralization-Line Technique for Wireless USB-Dongle Applications," *IEEE Trans. Antennas Propagat.*, vol. 60, no. 2, pp. 456–463, Feb. 2012, doi: 10.1109/TAP.2011.2173450.
- [19] A. N. Kulkarni and S. K. Sharma, "A multiband antenna with MIMO implementation for USB dongle size wireless devices," *Micro Opt. Tech. Lett.*, vol. 54, no. 8, pp. 1990–1994, Aug. 2012, doi: 10.1002/mop.26967.
- [20] S. Zhang, B. K. Lau, Y. Tan, Z. Ying, and S. He, "Mutual Coupling Reduction of Two PIFAs With a T-Shape Slot Impedance Transformer for MIMO Mobile Terminals," *IEEE Trans. Antennas Propagat.*, vol. 60, no. 3, pp. 1521–1531, Mar. 2012, doi: 10.1109/TAP.2011.2180329.
- [21] H.-X. Xu, G.-M. Wang, M.-Q. Qi, and H.-Y. Zeng, "Ultra-small single-negative electric metamaterials for electromagnetic coupling reduction of microstrip antenna array," *Opt. Express*, vol. 20, no. 20, Sep. 2012, Art. no. 21968, doi: 10.1364/OE.20.021968.
- [22] L. Y. Nie, X. Q. Lin, Z. Q. Yang, J. Zhang, and B. Wang, "Structure-Shared Planar UWB MIMO Antenna With High Isolation for Mobile Platform," *IEEE Trans. Antennas Propagat.*, vol. 67, no. 4, pp. 2735–2738, Apr. 2019, doi: 10.1109/TAP.2018.2889596.
- [23] W. Youcheng, Y. Yanjiao, C. Qingxi, and P. Hucheng, "Design of a compact ultra-wideband MIMO antenna," *J. Eng.*, vol. 2019, no. 20, pp. 6487–6489, Oct. 2019, doi: 10.1049/joe.2019.0277.
- [24] P. Sharma, R. N. Tiwari, P. Singh, P. Kumar, and B. K. Kanaujia, "MIMO Antennas: Design Approaches, Techniques and Applications," *Sensors*, vol. 22, no. 20, p. 7813, Oct. 2022, doi: 10.3390/s22207813.
- [25] S. Thiruvankadam and E. Parthasarathy, "Integrated Narrow Band (NB) and UWB MIMO Antenna for IoT Applications," *IETE J. Res.*, vol. 70, no. 4, pp. 3435–3446, Apr. 2024, doi: 10.1080/03772063.2023.2196260.
- [26] H. Taha Sediq, J. Nourinia, and C. Ghobadi, "A novel shaped antenna for designing UWB-MIMO system in microwave communications," *AEU - Int. J. Electron. Commun.*, vol. 152, p. 154249, Jul. 2022, doi: 10.1016/j.aeue.2022.154249.
- [27] S. Thiruvankadam, E. Parthasarathy, S. K. Palaniswamy, S. Kumar, and L. Wang, "Design and Performance Analysis of a Compact Planar MIMO Antenna for IoT Applications," *Sensors*, vol. 21, no. 23, Art. no. 7909, Nov. 2021, doi: 10.3390/s21237909.